

JET CROSS SECTIONS IN NNLO QCD IN LEPTON AND HADRON COLLISIONS

Gábor Somogyi

MTA-DE Particle Physics Research Group, 4010 Debrecen, PO Box 105, Hungary

Abstract

We present an overview of the main conceptual issues which arise when computing next-to-next-to-leading order perturbative corrections to jet cross sections in QCD. In particular we focus on the issue of infrared singularities that arise in intermediate steps of the calculation and outline the various methods which have been proposed to treat these divergences. We then give a brief overview of the state of the art of the field, concentrating on computations which deal strictly with the production of jets without additional electroweak or Higgs particles.

1 Introduction

The study of the production of hadronic jets in particle collisions played a crucial role in establishing QCD as the correct theory of strong interactions. Today, jet related studies continue to be important for improving our understanding of QCD. Indeed, jet rates and event shapes measured in three jet production in electron-positron annihilation are still among some of the most precise tools used for the extraction of the main parameter of the theory, the strong coupling α_s . Jet production at hadron colliders such the Tevatron and LHC can provide valuable information on the non-perturbative Parton Distribution Functions (PDF). Although the quark PDFs are significantly constrained by data from lepton-hadron Deep Inelastic Scattering (DIS) experiments such as HERA, the electrical neutrality of the gluon means that in DIS the gluon PDF can only be probed through specific final states (e.g., heavy quarks or jets) or indirectly through DGLAP evolution. In contrast, jet production at a hadron collider is directly sensitive to the gluon PDF, with LHC measurements already providing important constraints, in particular in the large- x region.

In addition to their role in determining Standard Model parameters, jets have also become essential analysis tools in searches for beyond the Standard Model physics. For example, “bump hunting” in the

dijet mass spectrum or testing the QCD running coupling at very large momentum transfer constitute powerful probes of BSM physics.

However, in order to fully exploit the physics potential of the wealth of available data, we must be able to calculate precise and reliable theoretical predictions for jet observables. Since the computation of physical quantities measured at particle colliders relies on the use of perturbation theory, one particular aspect of theoretical precision concerns the evaluation of exact higher-order corrections in perturbative QCD. As the numerical value of the strong coupling is not particularly small even at LHC energies, leading order (LO) results in QCD can only give an order of magnitude estimate of production rates and rough information on the shape of distributions. Furthermore, perturbative predictions depend on the non-physical renormalisation and factorisation scales and this dependence is usually quite sizeable at LO. Hence at least next-to-leading order (NLO) corrections must be evaluated. Nevertheless, in several situations, typically when NLO corrections are large, it is desirable to go even further in the perturbative expansion and include next-to-next-to-leading order (NNLO) corrections in our predictions.

In this contribution, we describe briefly the main conceptual difficulties in computing radiative corrections at NNLO accuracy in perturbative QCD as well as some approaches which have been proposed to overcome them. Then, we give a concise summary of the results available in the literature specifically for the production of jets at lepton and hadron colliders at NNLO accuracy.

2 Jet cross sections in NNLO QCD

At a hadron collider, the cross section for a given final state can be computed using the factorisation theorem,

$$d\sigma = \sum_{a,b} \int dx_a \int dx_b f_a(x_a, \mu_F^2) f_b(x_b, \mu_F^2) d\hat{\sigma}_{ab}(x_a, x_b, Q^2, \alpha_s(\mu_R^2)) + \mathcal{O}((\Lambda_{\text{QCD}}/Q)^m), \quad (1)$$

i.e., by convoluting the partonic cross section, $d\hat{\sigma}_{ab}$ with the PDFs f_a and f_b . (In lepton collisions, the PDFs are essentially Dirac delta functions, hence the convolution is trivial.) The PDFs are non-perturbative and must be extracted from data, however the partonic cross section can be evaluated in perturbation theory and we will focus on this aspect of the computation here. Since the basic issues that arise when computing the partonic cross section at higher orders are already present for the case of lepton collisions, we will present formulae appropriate to this simpler case in the following.

When computing QCD corrections to some specific partonic cross section, two conceptually separate issues must be addressed. The first concerns the evaluation of the matrix elements relevant to the process under study. At NNLO accuracy, we must consider up to two-loop corrections to the Born matrix element, one-loop matrix elements with one extra parton emission and tree level matrix elements with up to two extra parton emissions as compared to the Born process. These days the calculation of tree level matrix elements is essentially trivial and they can be computed in a completely automated way. Due to enormous progress in the past several years, by now also the evaluation of one-loop matrix elements has essentially been automated. While it should be said that the requirements on the numerical stability of one-loop amplitudes is more stringent in an NNLO calculation than an NLO one, this issue is being addressed by the newest generation of automated one-loop computations. Finally as regards the two-loop matrix elements, we recall that these have been available for some time for all $2 \rightarrow 2$ processes at the LHC (including the production of a vector boson pair, computed more recently) as well as for the production of three partons from a colourless initial state, relevant for electron-positron colliders. There is also a huge ongoing effort to move beyond these multiplicities and compute complete two-loop amplitudes relevant

for the production of three jets at the LHC or four jets at a lepton collider. (See e.g., ^{1, 2)} for some very recent examples.) While a great deal of progress has been made in this direction, the evaluation of two-loop amplitudes at high multiplicities currently remains a bottleneck.

Second, even if the relevant matrix elements are available, the computation of physical cross sections is not straightforward due to the presence of infrared and collinear singularities in intermediate stages of the calculation. In particular the finite NLO correction to some generic m -jet observable J is the sum of two terms, the real emission and virtual ones (J_n denotes the value of the observable J evaluated on an n -parton final state),

$$\sigma^{\text{NLO}} = \sigma_{m+1}^{\text{R}} + \sigma_m^{\text{V}} = \int_{m+1} d\sigma_{m+1}^{\text{R}} J_{m+1} + \int_m d\sigma_m^{\text{V}} J_m. \quad (2)$$

Both terms appearing above are separately divergent in $d = 4$ spacetime dimensions due to the presence of explicit ϵ poles from loop integrals (we use dimensional regularisation in $d = 4 - 2\epsilon$ dimensions) or phase space singularities associated with the emission of an unresolved parton. At NNLO accuracy we find that the complete NNLO correction is composed of three terms, the double-real, real-virtual and double-virtual ones,

$$\sigma^{\text{NNLO}} = \sigma_{m+2}^{\text{RR}} + \sigma_{m+1}^{\text{RV}} + \sigma_m^{\text{VV}} = \int_{m+2} d\sigma_{m+2}^{\text{RR}} J_{m+2} + \int_{m+1} d\sigma_{m+1}^{\text{RV}} J_{m+1} + \int_m d\sigma_m^{\text{VV}} J_m. \quad (3)$$

Again, the three pieces appearing above are all separately divergent in $d = 4$ dimensions due to the presence of explicit ϵ poles and/or phase space singularities which emerge in kinematic limits when one or two partons become unresolved. Although these divergences cancel for sufficiently inclusive (infrared and collinear safe) observables in the sum, in order to perform a numerical computation, this cancellation must be made explicit.

In broad terms, there have been two approaches to dealing with infrared and collinear singularities at NNLO: phase space slicing and the subtraction method. The slicing method relies on regularising the real emission phase space singularities with an explicit cut-off. With this cut-off in place, the real emission contribution is finite and can thus be computed numerically. On the other hand, the combination of the virtual contribution with the piece of the real contribution which has been discarded by the cut can be obtained from an appropriate resummation framework. This combination is also finite and can again be computed numerically. This procedure then regularises both real emission and virtual pieces, however an explicit cut-off parameter, δ , is introduced into the calculation. Since the rearrangement of terms in the slicing method is only exact for $\delta \rightarrow 0$, one must be careful to check that the results are independent (within numerical uncertainties) of the value of δ chosen. This can be challenging, since using a smaller value of δ generates a larger numerical cancellation between the regularised real and virtual contributions.

In practice, two types of such slicing methods have been employed to compute physical observables at NNLO accuracy, q_{T} slicing ³⁾ and N -jettiness slicing ^{4, 5)}. These methods use either the transverse momentum of the produced system, q_{T} , or the N -jettiness variable, τ_N , to disentangle “pure” NNLO regions in phase space, which are treated as explained above, while NLO type singularities are handled with some NLO subtraction method (see below).

On the other hand, the subtraction method makes use of approximate cross sections in order to perform an exact rearrangement of singular terms between the real and virtual contributions. At NLO accuracy one such approximate cross section is sufficient

$$\sigma^{\text{NLO}} = \int_{m+1} d\sigma_{m+1}^{\text{R}} J_{m+1} + \int_m d\sigma_m^{\text{V}} J_m = \int_{m+1} \left[d\sigma_{m+1}^{\text{R}} J_{m+1} - d\sigma_{m+1}^{\text{R},A_1} J_m \right]_{d=4} + \int_m \left[d\sigma_m^{\text{V}} J_m + \int_1 d\sigma_{m+1}^{\text{R},A_1} J_m \right]_{d=4}. \quad (4)$$

The approximate cross section $d\sigma_{m+1}^{\text{R},A_1}$ is constructed such that it has the same kinematic singularity structure (in d dimensions) as $d\sigma_{m+1}^{\text{R}}$ itself, hence the difference is free of non-integrable kinematic singularities and can be computed numerically with standard Monte Carlo methods. The poles of the virtual contribution, $d\sigma_m^{\text{V}}$, are then exactly cancelled by adding back the approximate cross section after integrating over the momentum and summing over the quantum numbers (colour, flavour) of the unresolved particle (these operations are all denoted by \int_1). Several explicit constructions are available in the literature for the approximate cross section $d\sigma_{m+1}^{\text{R},A_1}$ (6).

At NNLO accuracy this rearrangement is more involved due to the more elaborate structure of singularities. Since the double-real contribution has both single and double unresolved kinematic singularities, we write

$$\sigma_{m+2}^{\text{NNLO}} = \int_{m+2} \left\{ d\sigma_{m+2}^{\text{RR}} J_{m+2} - d\sigma_{m+2}^{\text{RR},A_2} J_m - \left[d\sigma_{m+2}^{\text{RR},A_1} J_{m+1} - d\sigma_{m+2}^{\text{RR},A_{12}} J_m \right] \right\}_{d=4}, \quad (5)$$

where $d\sigma_{m+2}^{\text{RR},A_2}$ regularises double unresolved singularities, while $d\sigma_{m+2}^{\text{RR},A_1}$ serves as a counterterm in single unresolved limits. The last term, $d\sigma_{m+2}^{\text{RR},A_{12}}$, is introduced to remove both the single unresolved singularities of $d\sigma_{m+2}^{\text{RR},A_2}$, as well as the double unresolved ones of $d\sigma_{m+2}^{\text{RR},A_1}$. Then, Eq. (5) is free of non-integrable singularities and can be computed with standard numerical methods.

The real-virtual contribution has both explicit ϵ -poles from one-loop amplitudes, as well as kinematic singularities associated with the emission of one extra parton as compared to the Born process. Thus we write

$$\sigma_{m+1}^{\text{NNLO}} = \int_{m+1} \left\{ \left[d\sigma_{m+1}^{\text{RV}} + \int_1 d\sigma_{m+2}^{\text{RR},A_1} \right] J_{m+1} - \left[d\sigma_{m+1}^{\text{RV},A_1} + \left(\int_1 d\sigma_{m+2}^{\text{RR},A_1} \right)^{A_1} \right] J_m \right\}_{d=4}. \quad (6)$$

The integrated form of the single unresolved subtraction from the double-real contribution, $\int_1 d\sigma_{m+2}^{\text{RR},A_1}$, precisely cancels the ϵ -poles of $d\sigma_{m+1}^{\text{RV}}$, however both terms are still singular in regions of phase space where one parton becomes unresolved. The task of the last two terms, $d\sigma_{m+1}^{\text{RV},A_1}$ and $\left(\int_1 d\sigma_{m+2}^{\text{RR},A_1} \right)^{A_1}$ is precisely the regularisation of these kinematic singularities. Hence, Eq. (6) is free of both ϵ -poles and non-integrable singularities and may be evaluated numerically.

Finally, the ϵ -poles of the double-virtual contribution are exactly cancelled by the sum of integrated counterterms which we have not yet added back,

$$\sigma_m^{\text{NNLO}} = \int_m \left\{ d\sigma_m^{\text{VV}} + \int_2 \left[d\sigma_{m+2}^{\text{RR},A_2} - d\sigma_{m+2}^{\text{RR},A_{12}} \right] + \int_1 \left[d\sigma_{m+1}^{\text{RV},A_1} + \left(\int_1 d\sigma_{m+2}^{\text{RR},A_1} \right)^{A_1} \right] \right\}_{d=4} J_m, \quad (7)$$

hence Eq. (7) is finite as guaranteed by the Kinoshita–Lee–Nauenber theorem and one can compute it numerically.

The construction of the approximate cross sections is not unique and indeed, several approaches exist in the literature for defining them such as iterated sector decomposition (7), antenna subtraction (8), sector improved residue subtraction (9), nested soft-collinear subtractions (10), the projection to Born technique (11) and the CoLoRFulNNLO scheme (12, 13, 14, 15).

3 Jet production at lepton colliders

As mentioned in the Introduction, the analysis of hadronic event shapes and jet rates at lepton colliders still provides one of the most precise ways to determine the value of the strong coupling α_s . Accordingly, these observables have been extensively measured in the past. In addition, the study of jet production in

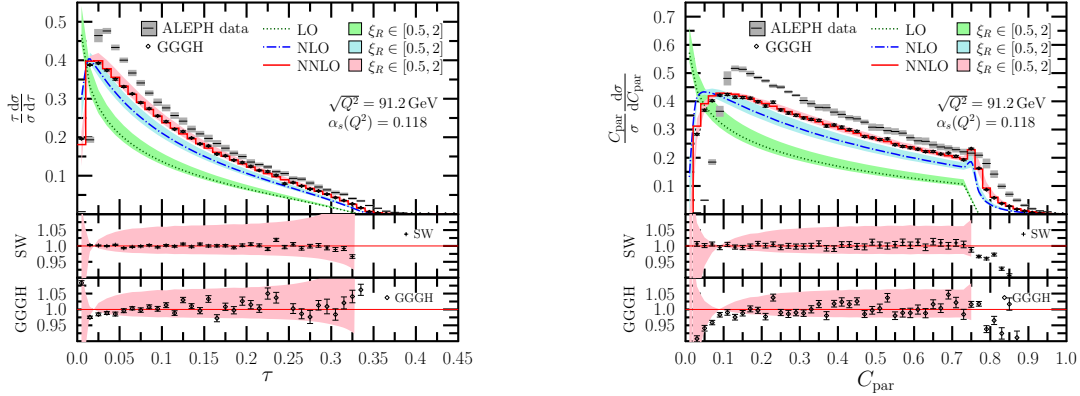


Figure 1: *Physical predictions for thrust ($\tau = 1 - T$) (left) and C -parameter (right) at LO, NLO and NNLO accuracy. The bands represent scale uncertainty. Data measured by the ALEPH collaboration is also shown. The lower panels show the ratio of predictions of ¹⁹⁾ (SW) and EERAD3 ²⁰⁾ (GGGH) to CoLoRFulNNLO.*

lepton collisions also serves as an ideal testing ground for developing tools and techniques for higher-order calculations in QCD.

Currently, the state of the art includes NLO predictions for the production of up to five jets ¹⁶⁾ (up to seven jets ¹⁷⁾ in the leading colour approximation) and NNLO predictions for the production of three jets ^{14, 15, 18, 19)}. In particular, the six standard event shapes measured in three jet production in electron-positron annihilation (thrust, heavy jet mass, total and wide jet broadening, C -parameter and the two-to-three jet transition variable y_{23} in the Durham jet clustering algorithm) have been computed at NNLO accuracy using both the antenna subtraction method ^{18, 19)} and the CoLoRFulNNLO subtraction scheme ¹⁵⁾. By way of illustration, we present in Fig.1 physical predictions for the distributions of thrust (T) and C -parameter up to NNLO accuracy at the LEP2 energy of $\sqrt{s} = 91.2$ GeV, computed in the CoLoRFulNNLO framework. The figures also show the comparison of these results to the predictions obtained with EERAD3 ²⁰⁾ (denoted as GGGH¹) as well with those of reference ¹⁹⁾ (denoted as SW²), both obtained with the antenna subtraction method. We observe a quite good agreement between the predictions of SW and CoLoRFulNNLO and a reasonably good agreement between GGGH and CoLoRFulNNLO. We note also the very good numerical convergence of the CoLoRFulNNLO method at NNLO.

Predictions for jet rates and event shapes computed at NNLO accuracy and supplemented with resummation, have been used to extract the strong coupling α_s from data (see ²¹⁾ for a review).

4 Jet production at hadron colliders

The computation of jet production at the LHC at NNLO accuracy, also in association with an electroweak or Higgs boson, is also of significant interest as discussed in the Introduction. Here we limit ourselves

¹We are grateful to G. Heinrich for providing the predictions of EERAD3 for us.

²In these comparisons we use updated (with respect to those published in ¹⁹⁾) but unpublished predictions provided to us by S. Weinzierl. We are grateful to S. Weinzierl for providing these updated results for us.

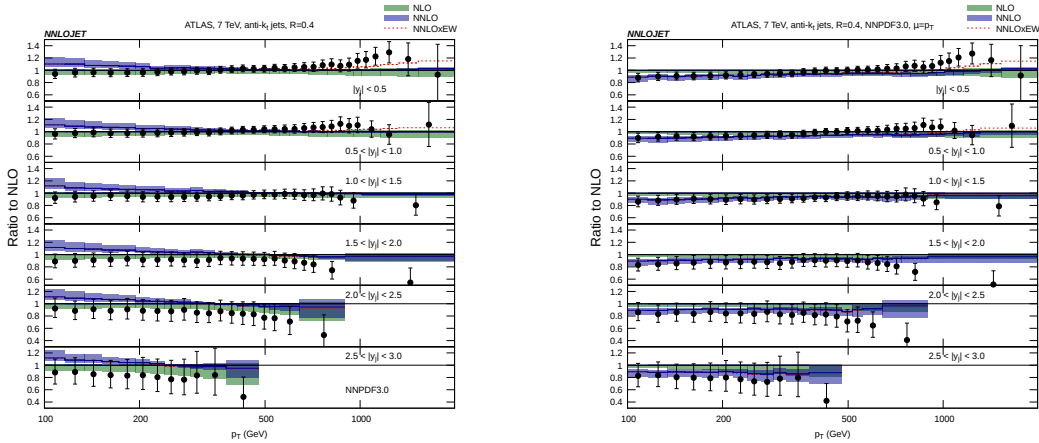


Figure 2: *Double-differential inclusive jet cross sections as a function of jet p_T in slices of rapidity form ²³⁾ (left) and ²⁴⁾ (right). The central scales are set to the transverse momentum of the leading jet, p_{T1} (left) or the individual jet p_T (right). The bands represent scale uncertainty.*

to discussing only those results which pertain strictly to the production of jets, without additional electroweak or Higgs particles. In this regard, the state of the art computations include NLO predictions for up to five jets in hadronic collisions ²²⁾, as well as the very recent NNLO predictions for single jet inclusive production ^{23, 24)} and dijet production ²⁵⁾. The NNLO computations have so far been obtained in the leading colour approximation, however they do include all partonic subprocesses. In each case, they have been computed within the antenna subtraction framework.

As an illustration, we present in Fig.2 double-differential results for the jet p_T in rapidity bins in single inclusive jet production at the 7 TeV LHC from references ²³⁾ and ²⁴⁾, together with data measured by the ATLAS collaboration. The jets in these computations are defined using the anti- k_t algorithm with a radius of $R = 0.4$. The left and right panels present predictions with two different choices of renormalisation and factorisation scales. On the left, the scales are set to the transverse momentum of the leading jet, p_{T1} , while on the right, they are set equal to the individual jet p_T . The bands represent the effects of varying $\mu = \mu_R = \mu_F$ by factors of 0.5 and 2 around the central value. We observe that overall the NNLO corrections are moderate and the two different scale choices are equivalent at large transverse momentum. However, at low transverse momentum, differences between the predictions emerge that are outside the scale band. Evidently the calculation based on the individual jet p_T provides a better description of data, however the fact that the two predictions deviate in excess of the scale band implies that further studies of scale setting are required.

We note that the first qualitative comparisons of these NNLO predictions with LHC data have already appeared in the literature ²⁶⁾.

5 Conclusions

In this contribution we discussed the state of the art with regards to computing QCD radiative corrections to jet cross sections in lepton and hadron collisions. These days, it is possible to compute these corrections at NNLO accuracy in QCD perturbation theory for the production of up to three jets in electron-positron annihilation and up to two jets in hadron collisions. After discussing the main conceptual issues that

must be addressed when going to NNLO, we gave brief illustrative examples of results obtained for event shape variables measured at LEP2 as well as for single inclusive jet production at the LHC.

6 Acknowledgements

The author is grateful to A. Kardos for useful discussions. This work was supported by grant K 125105 of the National Research, Development and Innovation Office in Hungary.

References

1. S. Badger, C. Brønnum-Hansen, H. B. Hartanto and T. Peraro, arXiv:1712.02229 [hep-ph].
2. D. Chicherin, J. Henn and V. Mitev, arXiv:1712.09610 [hep-th].
3. S. Catani and M. Grazzini, Phys. Rev. Lett. **98**, 222002 (2007)
4. J. Gaunt, M. Stahlhofen, F. J. Tackmann and J. R. Walsh, JHEP **1509**, 058 (2015)
5. R. Boughezal, C. Focke, X. Liu and F. Petriello, Phys. Rev. Lett. **115**, no. 6, 062002 (2015)
6. S. Frixione, Z. Kunszt and A. Signer, Nucl. Phys. B **467**, 399 (1996), S. Catani and M. H. Seymour, Nucl. Phys. B **485**, 291 (1997) Erratum: [Nucl. Phys. B **510**, 503 (1998)], G. Somogyi, JHEP **0905**, 016 (2009), C. H. Chung and T. Robens, Phys. Rev. D **87**, 074032 (2013)
7. T. Binoth and G. Heinrich, Nucl. Phys. B **585**, 741 (2000)
8. A. Gehrmann-De Ridder, T. Gehrmann and E. W. N. Glover, JHEP **0509**, 056 (2005)
9. M. Czakon, Phys. Lett. B **693**, 259 (2010)
10. F. Caola, K. Melnikov and R. Rntsch, Eur. Phys. J. C **77**, no. 4, 248 (2017)
11. M. Cacciari, F. A. Dreyer, A. Karlberg, G. P. Salam and G. Zanderighi, Phys. Rev. Lett. **115**, no. 8, 082002 (2015)
12. G. Somogyi, Z. Trócsányi and V. Del Duca, JHEP **0701**, 070 (2007)
13. G. Somogyi and Z. Trócsányi, JHEP **0701**, 052 (2007)
14. V. Del Duca, C. Duhr, A. Kardos, G. Somogyi and Z. Trócsányi, Phys. Rev. Lett. **117**, no. 15, 152004 (2016)
15. V. Del Duca, C. Duhr, A. Kardos, G. Somogyi, Z. Szőr, Z. Trócsányi and Z. Tulipánt, Phys. Rev. D **94**, no. 7, 074019 (2016)
16. R. Frederix, S. Frixione, K. Melnikov and G. Zanderighi, JHEP **1011**, 050 (2010)
17. S. Becker, D. Goetz, C. Reuschle, C. Schwan and S. Weinzierl, Phys. Rev. Lett. **108**, 032005 (2012)
18. A. Gehrmann-De Ridder, T. Gehrmann, E. W. N. Glover and G. Heinrich, JHEP **0712**, 094 (2007)
19. S. Weinzierl, JHEP **0906**, 041 (2009)

20. A. Gehrmann-De Ridder, T. Gehrmann, E. W. N. Glover and G. Heinrich, *Comput. Phys. Commun.* **185**, 3331 (2014)
21. C. Patrignani *et al.* [Particle Data Group], *Chin. Phys. C* **40**, no. 10, 100001 (2016).
22. Z. Bern *et al.*, *Phys. Rev. Lett.* **109**, 042001 (2012), S. Badger, B. Biedermann, P. Uwer and V. Yundin, *Phys. Lett. B* **718**, 965 (2013), S. Badger, B. Biedermann, P. Uwer and V. Yundin, *Phys. Rev. D* **89**, no. 3, 034019 (2014)
23. J. Currie, E. W. N. Glover and J. Pires, *Phys. Rev. Lett.* **118**, no. 7, 072002 (2017)
24. J. Currie, E. W. N. Glover, T. Gehrmann, A. Gehrmann-De Ridder, A. Huss and J. Pires, *Acta Phys. Polon. B* **48**, 955 (2017)
25. J. Currie, A. Gehrmann-De Ridder, T. Gehrmann, E. W. N. Glover, A. Huss and J. Pires, *Phys. Rev. Lett.* **119**, no. 15, 152001 (2017)
26. M. Aaboud *et al.* [ATLAS Collaboration], arXiv:1711.02692 [hep-ex].